AUT Journal of Mechanical Engineering

AUT J. Mech. Eng., 6(2) (2022) 189-200
DOI: 10.22060/ajme.2021.20455.6004

Synthesis of a Six-Link Mechanism for Generating the Ankle Motion Trajectory Using Shadow Robot Control Method

A. Vali [1], M. R. Haghjoo [2], B. Beigzadeh[1]*

[1] Biomechatronics and Cognitive Engineering Research Lab, School of Mechanical Engineering, Iran University of Science and Technology, Iran

[2] Department of Mechanical Engineering, Shahid Beheshti University, Tehran, Iran

ABSTRACT: In this paper, one degree of freedom Stephenson type III mechanism is synthesized to generate the human ankle gait trajectory by considering prescribed timing. The produced trajectory must be consistent with the natural motion of the human foot in terms of position and timing. In this regard, we used the robust and effective shadow robot algorithm that synthesizes the mechanism's dimensions and considers prescribed timing, which is a crucial topic in gait rehabilitation devices. In this method, a mechanism with multiple fixed links is replaced by a hypothetical equivalent shadow robot with several degrees of freedom. Then, optimizing a suitable controller for the shadow robot leads to finding optimal mechanism dimensions. Afterward, the adjustability of this mechanism for generating other similar ankle gait trajectories is shown. Adjustability has been accomplished through the little change in the crank and coupler link sizes. The optimized mechanism generates ankle movement for different people with different leg lengths and has the least spatial and timing error. The reasonable error confirms the usage of the mechanism in gait rehabilitation devices.

Review History:

Received: Aug. 26, 2021
Revised: Dec. 05, 2021
Accepted: Dec. 21, 2021
Available Online: Dec. 28, 2021

Keywords:

Mechanism synthesis
Six-link
Stephenson mechanism
Ankle trajectory
Gait rehabilitation

1- Introduction

As the global average age increases, the need for exercises to help people recover or rehabilitate their walking ability increases. Robots can help us cope with this by evaluating the patient's performance and providing the desired treatments [2, 3]. Rehabilitation robots can be used to restore lost abilities and facilitate daily activities [4]. For example, Exoskeletons are a group of wearable rehabilitation robots that can exchange forces and information between the person and the mechanism due to the physical contact between the person and the device. These mechanisms may play an auxiliary role or act instead of a disabled limb [5, 6].

One of the best ways to rehabilitate the lower extremities is to use mechanisms with one degree of freedom. These mechanisms are easy to use and perform a repetitive operation with excellent safety and lower price than conventional physical rehabilitation and most current commercial solutions [7-10]. It is noteworthy that considering a higher safety factor is crucial for robots directly interacting with humans [11]. 1 Degree of Freedom (DOF) mechanized gait trainers employing linkage mechanisms can imitate the gait trajectory of the human user at a potentially lower cost than current commercial solutions [8]. Four-link, six-link, and eight-link mechanisms are three possible candidates for 1DOF mechanisms. Among them, provided by several studies, the four-link mechanism is not capable of generating the prescribed timing of complicated trajectories like ankle trajectory [10, 12-14]. One type of eight-link mechanism called the Jansen mechanism was recently synthesized in Ref. [9] and [15] to generate gait ankle trajectory for gait rehabilitation. However, due to the high number of linkages and high inertia of an eight-link mechanism, it seems too bulky for a gait rehabilitation purpose. The Jansen mechanism has eight links and ten joints, so a six-link mechanism like Stephenson III with fewer links and the ability to generate complicated trajectories can be a wise choice for gait rehabilitation devices.

The six-link mechanism is a 1DOF mechanism that consists of six links and seven joints and has two separate topological configurations. These two topologies are called Watt and Stephenson [16]. Stephenson III is one of the inversions of the Stephenson mechanism. This mechanism has been used a few times in rehabilitation devices to guide the natural walking movement, but the prescribed timing is not considered in studies [8, 9, 17]. It can be concluded from the literature that the synthesis of path-generating mechanisms is challenging, especially when prescribed timing is being considered [10]. When synthesizing the mechanism for a rehabilitation device, it is important to consider prescribed timing. The mechanism should have the least possible error in terms of time and space; even the timing error must be more concerned than spatial error. In a four-link mechanism, up to

*Corresponding author's email: b_beigzadeh@iust.ac.ir

5 precision points can be guaranteed considering prescribed timing, and nine precision points can be considered without consideration of prescribed timing in analytical synthesizing methods [18, 19]. Therefore, a suitable solution is needed to ensure the accuracy of path generation and reduce errors. In this regard, lots of effort has been made to take advantage of global optimization algorithms [19-22]. An objective function called "structural error" is commonly used in literature. This function obtains the summation of the distance mean-squares between the desired and generated trajectory [23, 24]. However, Finding the global optimization of this function is not straightforward due to its being multimodal and nonlinear and the dependence of the optimization results on the initial values [25]. For this reason, more effective alternatives to this objective function are proposed in the literature, like orthogonal arrays, cyclic angular deviation, and normalized Fourier descriptors [26-28]. Recently, a method for synthesizing the optimal path of mechanisms with prescribed timing has been introduced in reference [10] named shadow robot algorithm based on optimal trajectory tracking control theory. The shadow robot algorithm has the advantage of being robust and minimizing time and spatial errors simultaneously and strikes a balance between timing and spatial errors. However, this effective method has not been developed for the case of six-link mechanisms yet.

Hence, the contribution of this research is: the shadow robot method is developed for synthesizing the six-link Stephenson type III mechanism. Further, this six-link mechanism is optimized to generate the human ankle trajectory during a natural gait, considering its position and prescribed timing.

The structure of this article is as follows: in the next section, the formulation related to the problem is discussed, and the Stephenson mechanism's dimensions are sought using the shadow robot method. In the third section, the results are shown and discussed. In the fourth section, the conclusions are presented.

2- Problem Formulation

This section presents the problem formulation, and the details of the proposed method for path synthesizing are described.

2- 1- Dimensional synthesis (optimization)

The parameters of the Stephenson III mechanism are shown in Fig. 1. The mechanism coupler point, i.e., point c, is considered as the ankle joint, and the hip is considered as the reference coordinate system for the path synthesis. Point O represents the hip joint place, which is connected to the fixed link of the mechanism (link l_1). Vector $\hat{\mathbf{c}}$ indicates the location of the coupler point c relative to the hip joint O. The location of the coupler point c at each time can be displayed using a nonlinear function of $\hat{\mathbf{x}}$ and θ_2 as follows [10]:

$$\hat{\mathbf{c}} = f\left(\hat{\mathbf{x}}, \theta_2\right) \tag{1}$$

When the mechanism has six links, $\hat{\mathbf{x}}$ contains 15 parameters, these parameters can be displayed as $\hat{\mathbf{x}} = \left[x_0, y_0, x'_0, y'_0, \theta_0, l_1, l_2, l_3, l_4, l_{5x}, l_{5y}, l'_2, l'_{5x}, l'_{5y}, l'_6\right]$ which can be seen in Fig. 1, and θ_2 refers to the angle of the crank input as a function of the time. Over time, the coupler link follows the trajectory $\hat{\mathbf{c}}(t)$. Attempts are made to make $\hat{\mathbf{c}}(t)$ match the desired trajectory $\hat{\mathbf{c}}_{\mathbf{d}}(t)$ as much as possible. In Eq. (1), the location of the coupler point can be written as [10]:

$$\hat{\mathbf{c}} = \begin{bmatrix} c_x \\ c_y \end{bmatrix} = \begin{bmatrix} \cos\theta_0 & -\sin\theta_0 \\ \sin\theta_0 & \cos\theta_0 \end{bmatrix} \hat{c}_L + \begin{bmatrix} x_0 \\ y_0 \end{bmatrix} \tag{2}$$

In this equation, $\hat{\mathbf{c}}_{\mathbf{L}}$ shows the coupler point's location in local coordination $\mathbf{X_L Y_L}$ shown in Fig. 1; And is defined as Eq. (3).

$$\begin{gathered} \hat{\mathbf{c}}_{\mathrm{L}} = l'_2 \begin{bmatrix} \cos\theta'_2 \\ \sin\theta'_2 \end{bmatrix} + \begin{bmatrix} \cos\theta'_3 & -\sin\theta'_3 \\ \sin\theta'_3 & \cos\theta'_3 \end{bmatrix} \begin{bmatrix} l'_{5x} \\ l'_{5y} \end{bmatrix} = \\ \begin{bmatrix} l'_2 \cos\theta'_2 + l'_{5x} \cos\theta'_3 - l'_{5y} \sin\theta'_3 \\ l'_2 \sin\theta'_2 + l'_{5x} \sin\theta'_3 + l'_{5y} \cos\theta'_3 \end{bmatrix} \end{gathered} \tag{3}$$

θ'_2 is the angle between l'_2 and $\mathbf{X_L}$, and θ'_3 is the angle between l'_{5x} with $\mathbf{X_L}$.

The walking kinematic data from healthy subjects at low speeds are collected to define the desired trajectory [29, 30]. This data reports the angles of the hip and knee joints during gait at averaged speed normalized by the subject's height (speed divided by 0.49 height per second). Angles shown in Fig. 6 are used to obtain the ankle trajectory [31, 32]. This calculation does not discuss the foot's orientation or the ankle angle (the ankle angle is not directly controlled in this device). Any angle of the crank in terms of time is named as $\theta_2(i)$ and corresponds to one of desired trajectory point $\hat{\mathbf{c}}_{\mathbf{d}}(i)$, and $\theta_2(i) = \frac{2\pi}{100}(i-1)$ for $i = 1, \cdots, 100$, having one hundred constant increments for the complete rotation of the crankshaft because the normalized elapsed time between two consecutive points on the desired trajectory is considered equal to 1% of the gait cycle .Note that the rotational speed of the crankshaft is deemed to be constant.

2- 2- Standardizing

To compare the desired trajectory c_d with the generated trajectory, each should be standardized as described in Ref. [10] and shown in Fig. 2 .The standardizing procedure

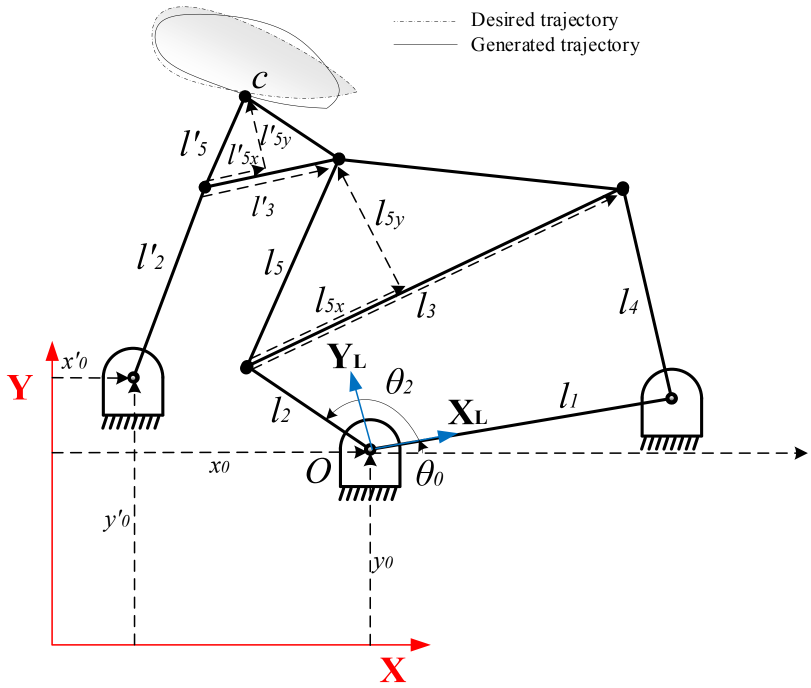

Fig. 1. Stephenson III mechanism design parameters. O is the hip joint location, which is connected to the mechanism's fixed link. c indicates the ankle point.

contains correcting the traveling direction meaning that if the trajectory's traveling direction is clockwise (regardless of the crankshaft rotation direction), it should be reversed and changed to a counterclockwise rotating direction. Note that the starting point is considered as the farthest point from the trajectory's geometric center, which is shown in Fig. 2 as P_m. Also, the geometric center of the trajectory is obtained by Eq. (4).

$$\mathbf{P}_{[c]} = \frac{1}{N}\sum_{i=1}^{N}\mathbf{c}(i) \tag{4}$$

The desired trajectory must be standardized at the beginning, and the generated trajectory must be standardized at the beginning of each algorithm iteration.

2- 3- Constraints

Boundary values and inequality constraints are the main constraints on the dimensions. Each of the dimensions of the mechanism must be within an acceptable range for design:

$$\begin{aligned} & x_{k,\min} \le x_k \le x_{k,\max} \\ & x_k \in \mathbf{x} = \\ & \left[x_0, y_0, x_0^{'}, y_0^{'}, \theta_0, l_1, l_2, l_3, l_4, l_{5x}, l_{5y}, l_2^{'}, l_{5x}^{'}, l_{5y}^{'}, l_6^{'}\right] \end{aligned} \tag{5}$$

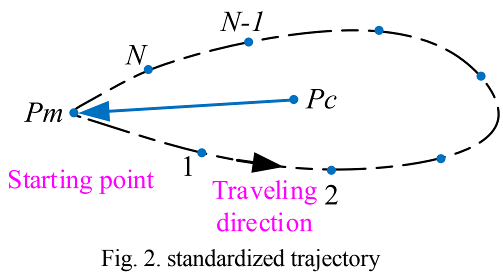

Fig. 2. standardized trajectory

Also, Grashof inequality constraints are considered as Eq. (6).

$$\begin{aligned} & g(l_1, l_2, l_3, l_4) := \\ & 2\left(\min(l_1, l_2, l_3, l_4) + \max\left(l_1, l_2, l_3, l_4\right)\right) - \\ & \left(l_1, l_2, l_3, l_4\right) < 0 \end{aligned} \tag{6}$$

To consider these constraints, Eq. (7) is added to the

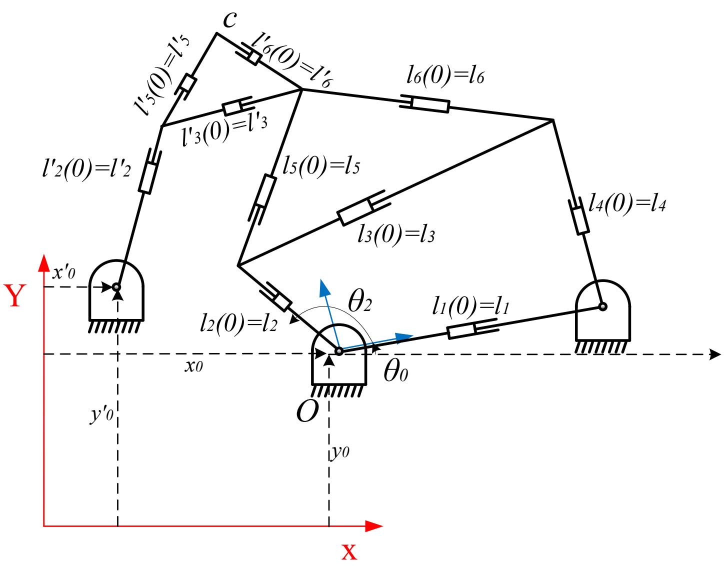

Fig. 3. Shadow robot equivalent to Stephenson III mechanism

equation of the main objective function, in which M is selected as the penalty coefficient and has a large positive value.

$$P = M \max\left(g, 0\right) \tag{7}$$

If several inequality constraints are required, in Eq. (7), g is replaced by $g_n\left(n = 1, 2\ldots\right)$. This penalty function is more efficient than penalty functions such as $p = M * h\left(h = 0 or 1\right)$ used in some studies because the value of such functions increases suddenly once g is getting close to the boundary of the inequality (unlike the function provided here, in which the process of change is gradual).

2- 4- bjective function

It is necessary to study the shadow robot equivalent to the corresponding mechanism to propose the objective function. This robot is shown in Fig. 3. The shadow robot is defined by several degrees of freedom, which is quite similar to the original mechanism, except that all of the fixed parameters labeled as $\mathbf{x}$ in the initial mechanism are replaced with variable actuators labeled as $\tilde{\mathbf{x}}\left(t\right)$. Each actuator in the initial condition is considered equal to the mechanism's corresponding parameters ($\tilde{\mathbf{x}}\left(0\right) = \mathbf{x}$).

According to the control theory, the robot control effort during tracking decreases as long as the function in Eq. (8) minimizes [10].

$$j = \int_0^{t_f} \mathbf{u}\left(t\right)^T \mathbf{w}\left(t\right)\mathbf{u}\left(t\right)dt \ or \ \int_0^{t_f} \left\|\mathbf{u}\left(t\right)\right\|^2 w\left(t\right)dt \tag{8}$$

In this function, $\mathbf{u}$ is the control signal, $\mathbf{w}$ is the weight matrix and is a symmetric positive definite matrix, t_f is the last time we follow the desired trajectory, and $\left\|.\right\|$ indicates the second norm of the vector . $\mathbf{u}$ consists of two independent hypothetical forces and can be represented as $\begin{bmatrix} u_x \\ u_y \end{bmatrix}$. $\mathbf{w}$ in general form is represented as $\begin{bmatrix} w_x & w_{xy} \\ w_{xy} & w_y \end{bmatrix}$. In this paper, $\mathbf{w}$ is considered to be diagonal, and the values on the main diagonal are deemed to be equal. Finally, by ignoring the power of 2 for $\left\|\mathbf{u}\left(t\right)\right\|$ for simplification, we get to the following equation [10]:

$$J = \int_0^{t_f} w\left(t\right)\left\|\mathbf{u}\left(t\right)\right\|dt \tag{9}$$

Considering the contour error mentioned in the reference [10] and the placement of the Proportional Derivative (PD) controller for the mechanism:

Table 1. Boundary Values

	The minimum value (mm)	The maximum value (mm)
l_1	0.1	800
l_2	0.1	400
l_3	0.1	800
l_4	0.1	800
l_{5x}	-800	800
l_{5y}	-800	800
l'_2	0.1	800
l'_3	0.1	800
l'_{5x}	-800	800
l'_{5y}	-800	800
x_0	-800	800
y_0	-800	800
x'_0	-800	800
y'_0	-800	800
Θ_0	-π	π

$$\mathbf{u} = \mathbf{e_c} + T_v \dot{\mathbf{e}}_\mathbf{c} \tag{10}$$

In this equation, $\mathbf{e_c}$ is the contour error and is the shortest distance between the desired and generated trajectories, and T_v is the derivative time constant.

After replacing the equation u in Eq. (9) by using Eq. (10) [10]:

$$J = \int_0^{t_f} w(t)\|\mathbf{u}(t)\|dt = \int_0^{t_f} w(t)\|\mathbf{e_c}(t) + T_v \dot{\mathbf{e}}_\mathbf{c}(t)\|dt \tag{11}$$

Therefore, taking constraints of inequality into account, the objective function can be written as [10]:

$$Jo = \sum_{i=1}^{N} w(i)\|\mathbf{u}(i)\| + M \max(g,0) = \sum_{i=1}^{N} w(i)\|\mathbf{e_c}(i) + T_v \dot{\mathbf{e}}_\mathbf{c}(i)\| + M \max(g,0) \tag{12}$$

The contour error in this equation is calculated as follows [10]:

In general, $0 < \Delta \le 0.2N$,in which N is the trajectory's total number of considered points.

2- 5- Global optimization algorithm

The global optimization algorithm specifically uses the initial condition $\mathbf{x_0}$ to create $j-1$ starting points randomly. These j initial points are distributed over the boundaries. Then, local minimums are found by starting from the generated initial points and using a typical local solver, such as the gradient descent algorithm. A global minimum is found by choosing a sufficiently high number of local starting points. Fmincon is provided as a nonlinear programming solver in Matlab's Optimization Toolbox. This powerful solver can be used instead of the gradient descent algorithm. The Multi-start option in Matlab gives the ability to have j initial points.

3- Results and Discussion

Optimal dimensions of the Stephenson III mechanism are sought using the shadow robot algorithm described above. The gait desired trajectory is obtained using an available kinematics database collected for low-speed walking in Refs. [29, 30]. The boundary conditions for optimization are considered in Table 1 as mentioned in Section 2.3.

Table 2 contains the optimized dimensions of the mechanism obtained by using the shadow robot algorithm. Given these values, the mechanism is shown at the starting

$$\mathbf{e_c}(i) \cong \begin{cases} \min\left(\mathbf{c_d}(j) - \mathbf{c}(i)\right) \quad for \quad j \in \left[i - \frac{\Delta}{2}, i + \frac{\Delta}{2}\right] & if \quad g \le 0 \quad or \quad \max(g,0) = 0 \\ \mathbf{c_d}(i) & if \quad g > 0 \quad or \quad \max(g,0) \ne 0 \end{cases} \tag{13}$$

Table 2. optimal values

	Optimal value (mm)
l_1	181.12
l_2	99.16
l_3	514.73
l_4	463.17
l_{5x}	327.87
l_{5y}	-705.58
l'_2	837.73
l'_3	989.59
l'_{5x}	755.82
l'_{5y}	-759.77
x_0	-358.06
y_0	179.84
x'_0	-193.79
y'_0	930.85
Θ_0	2.433

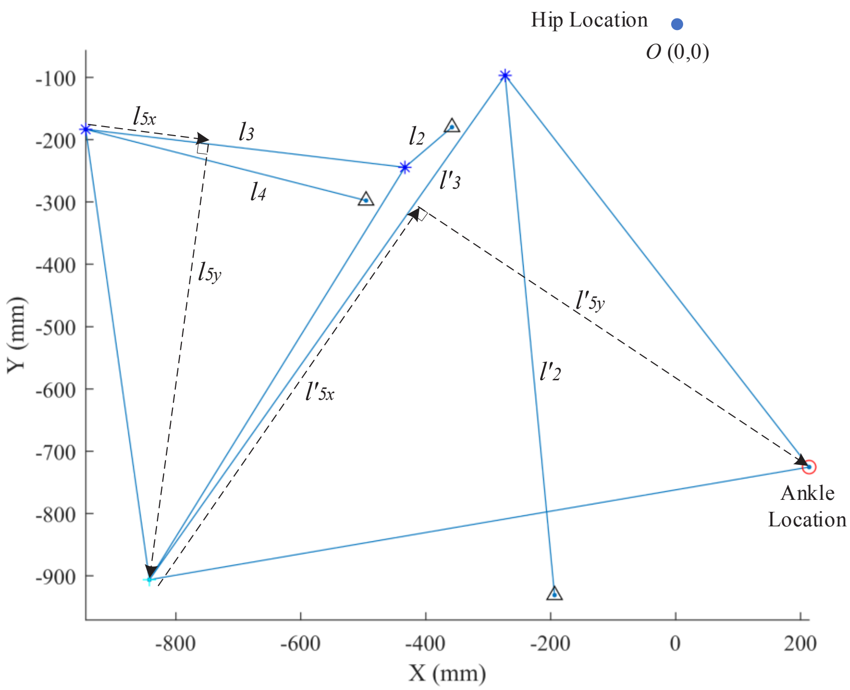

Fig. 4. Mechanism with dimensions optimized by shadow robot algorithm

point in Fig. 4.

As the presentation of 3D models helps to understand the application of the mechanism in rehabilitation devices, a simple Computer-Aided Design (CAD) model is presented in Fig. 5 for the mechanism connected to the right leg. A wooden doll is used as the human beside the right-hand side mechanism (the left-hand mechanism is the same as the right one, but it is not shown in the figure for the sake of clarity)

Five thousand starting points are used to find the optimal global values with the aid of the shadow robot algorithm (m = 5000). The time window for the contour error is $0.1N$ $\left(\Delta = 0.1N\right)$ .After optimizing the dimensions of the mechanism, the mechanism follows the desired trajectory, as is shown in Fig. 6. The points marked with circles are related to the trajectory produced by the mechanism, and the points marked with asterisks are related to the desired trajectory.

The rehabilitation device should be used to teach walking to different people. For this reason, it should be adjustable for

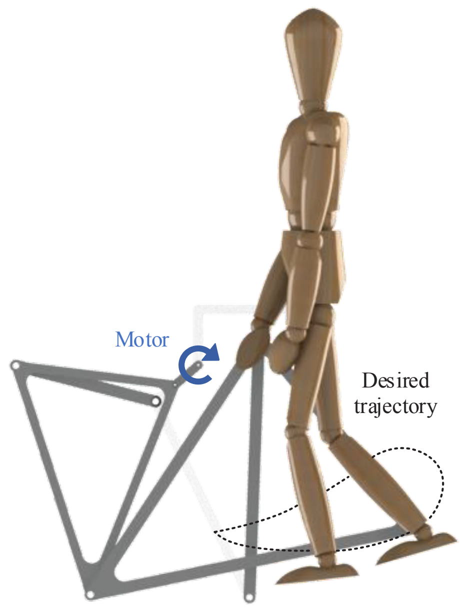

Fig. 5. Schematic of gait rehabilitation device with an optimized mechanism

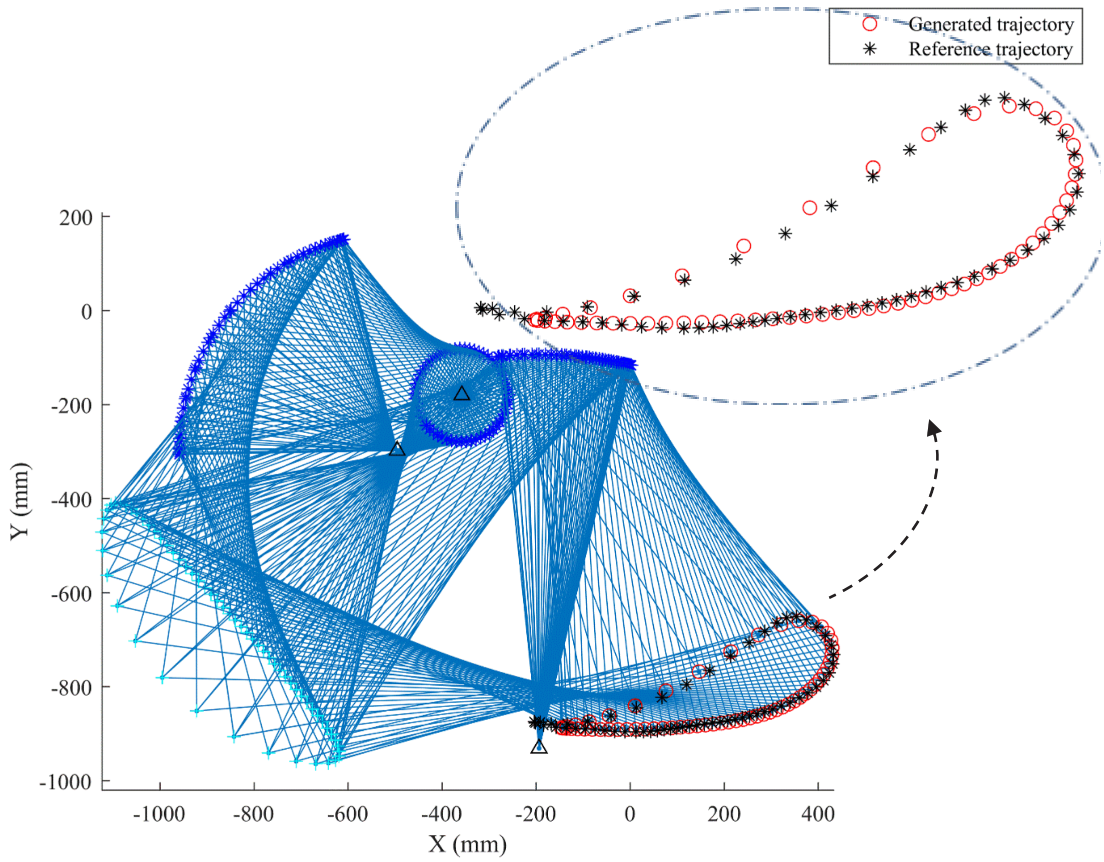

Fig. 6. Stephenson III's stick diagram optimized during crankshaft rotation

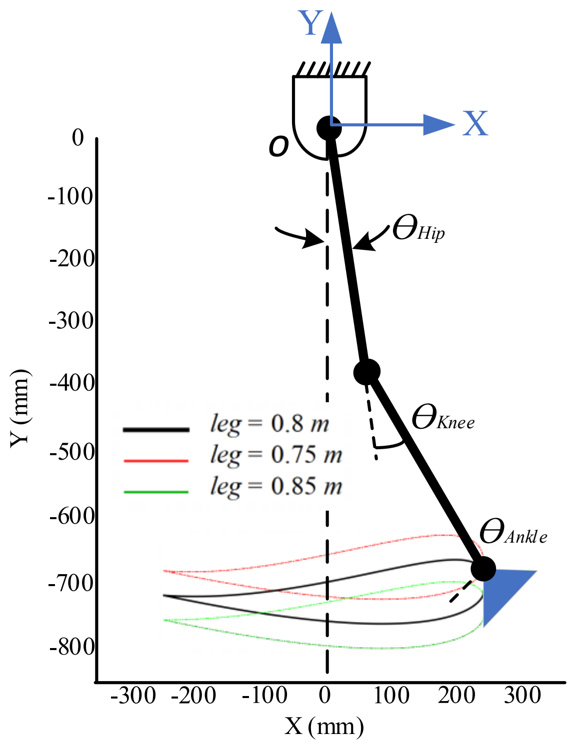

Fig. 7. The optimal trajectory for the ankle is obtained using the angles of the hip and knee joints [1].

different sizes, and several parameters should be considered variable. This device interacts with only two extremities of the leg, the ankle, and the hip, and does not interact with points between these two, such as the knee joint, shank, or thigh. Therefore, the only factor related to the body in this study is the leg's total length. As can be seen in the two-link model of Fig. 7, the change in the overall length of the link causes vertical displacement, along with a small change in the relative ankle trajectory scaling in the sagittal plane. Orientation and the net shape of the desired trajectory remain unchanged. Therefore, some design parameters are changeable to adjust the mechanism for different leg lengths. These parameters are explained below [1].

As shown in Fig. 1, the parameters x_0 and y_0 give us the mechanism's location relative to the hip in the sagittal plane. Changes in these parameters do not affect the path's orientation or shape; it represents the horizontal and vertical transmission of the trajectory in the sagittal plane [1].

The coupler length parameter l'_{5y} is another parameter that can make the mechanism adjustable by changing the location of the ankle. As shown in Fig. 8a, the change in l'_{5y} leads to the transmission of the trajectory relative to the origin.

For more precise adjustment, the length of the crank l_2 can be changed. As shown in Fig. 8b, this change affects the scale of the final path synthesis. All these parameter changes can be used to make the mechanism more adjustable for users.

4- Conclusion

In this paper, the dimensions of a 1 DOF Stephenson III robot are sought using the shadow robot method for generating ankle relative to hip trajectory. The Shadow robot algorithm is a robust and powerful synthesizing method considering prescribed timing. In this method, the mechanism with fixed-length links is replaced by the shadow robot with variable-length links or actuators. The objective function is obtained by minimizing the control effort and searching for the shadow robot optimal tracking controller. An existing global optimization technique is adopted to minimize the objective function considering relevant constraints. The adjustability of the mechanism is proved by changing the lengths of the crank and coupler links.

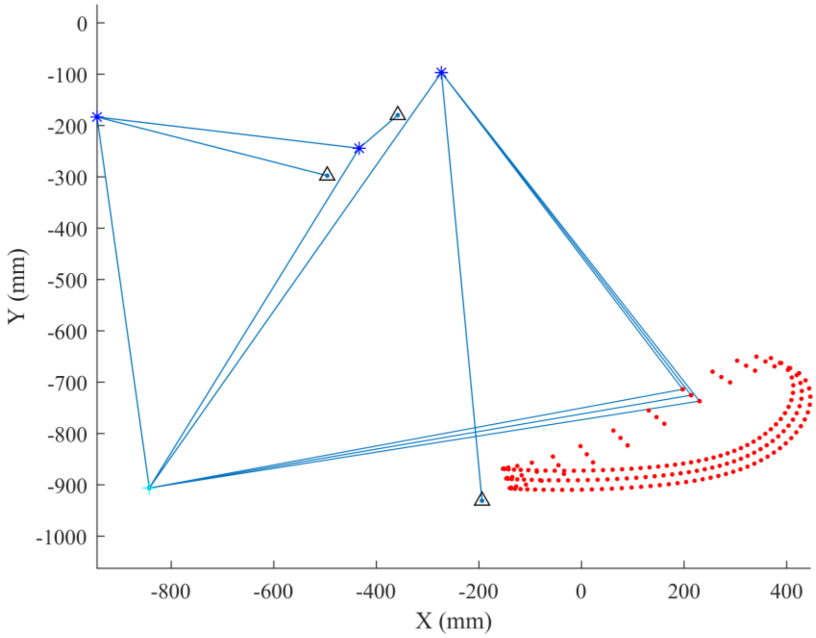

(a)

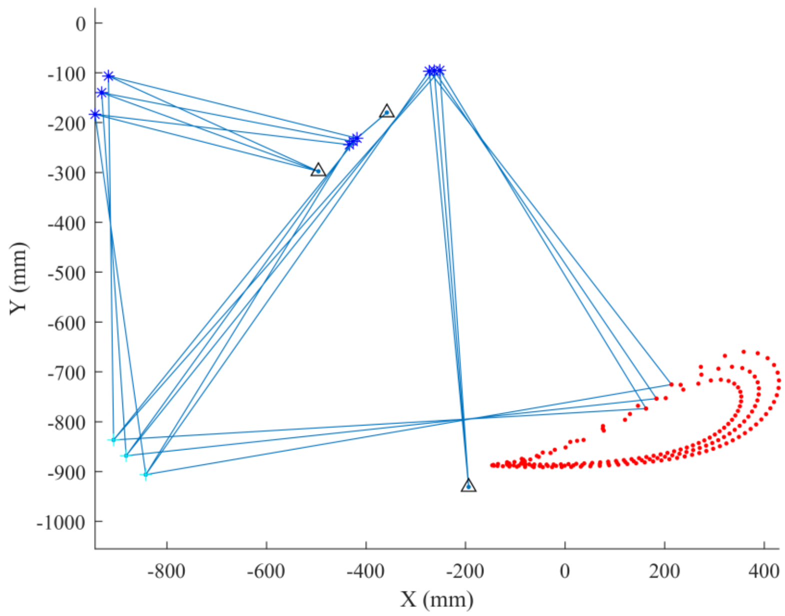

(b)

Fig. 8. The trajectory changes by adjusting a) l'_{5y} b) l_2

References

[1] M.R. Sabaapour, H. Lee, M.R. Afzal, A. Eizad, J. Yoon, Development of a Novel Gait Rehabilitation Device with Hip Interaction and a Single DOF Mechanism, (2019) 1492-1498.

[2] G.C. Henderson, J. Ueda, Pneumatically powered robotic exercise device to induce a specific force profile in target lower extremity muscles, Robotica, 32(8) (2014) 1281-1299.

[3] H.I. Krebs, B.T. Volpe, M.L. Aisen, W. Hening, S. Adamovich, H. Poizner, K. Subrahmanyan, N. Hogan, Robotic applications in neuromotor rehabilitation, Robotica, 21(1) (2003) 3-11.

[4] M. Kassler, Robotics for health care: a review of the literature, Robotica, 11(6) (1993) 495-516.

[5] B. Beigzadeh, M. Ilami, S. Najafian, Design and development of one degree of freedom upper limb exoskeleton, in: 2015 3rd RSI International Conference on Robotics and Mechatronics (ICROM), 2015, pp. 223-228.

[6] D. Martelli, F. Vannetti, M. Cortese, P. Tropea, F. Giovacchini, S. Micera, V. Monaco, N. Vitiello, The effects on biomechanics of walking and balance recovery in a novel pelvis exoskeleton during zero-torque control, Robotica, 32(8) (2014) 1317-1330.

[7] M.R. Haghjoo, J. Yoon, Two-stage mechanism path synthesis using optimized control of a shadow robot: Case study of the eight-bar Jansen mechanism, Mechanism and Machine Theory, 168(October 2021) (2022) 104569-104569.

[8] J. Lee, L. Li, S. Yul, A.D. Deshpande, Kinematic comparison of single degree-of-freedom robotic gait trainers Kinematic comparison of single degree-of-freedom robotic gait trainers, Mechanism and Machine Theory, 159(February) (2021) 104258-104258.

[9] M. Li, J. Yan, H. Zhao, G. Ma, Y. Li, Mechanically Assisted Neurorehabilitation: A Novel Six-Bar Linkage Mechanism for Gait Rehabilitation, IEEE Transactions on Neural Systems and Rehabilitation Engineering, 29 (2021) 985-992.

[10] M.R. Sabaapour, J. Yoon, A novel method for optimal path synthesis of mechanisms based on tracking control of shadow robot, Mechanism and Machine Theory, 131 (2019) 218-233.

[11] A.A. Mohammadi Nasrabadi, F. Absalan, S.A.A. Moosavian, Design, modeling and simulation of weight compensation walking assistant robot, Modares Mechanical Engineering, 17(5) (2017) 41-51.

[12] M.R. Haghjoo, H. Lee, M.R. Afzal, A. Eizad, J. Yoon, Mech-Walker : A Novel Single-DOF Linkage Device with Movable-Frame for Gait Rehabilitation, 1(c) (2020).

[13] W.-y.Y. Lin, Optimum path synthesis of a geared five-bar mechanism, Advances in Mechanical Engineering, 2013(Dcc) (2013).

[14] S.Y. Shin, A.D. Deshpande, J. Sulzer, Design of a single degree-of-freedom, adaptable electromechanical gait trainer for people with neurological injury, Journal of Mechanisms and Robotics, 10(4) (2018) 044503-044503.

[15] D.S.M. Varma, Synthesis and Analysis of Jansen's Leg-Based Mechanism for Gait Rehabilitation, in: D. Sen, S. Mohan, G.K. Ananthasuresh (Eds.) Mechanism and Machine Science, Springer Singapore, Singapore, 2021, pp. 303-315.

[16] J.M. McCarthy, G.S. Soh, Geometric Design of Linkages, in, 2011, pp. 1-14.

[17] B.Y. Tsuge, J.M. McCarthy, An adjustable single degree-of-freedom system to guide natural walking movement for rehabilitation, Journal of Medical Devices, Transactions of the ASME, 10(4) (2016) 044501-044501.

[18] C.W. Wampler, A.P. Morgan, A.J. Sommese, Complete solution of the nine-point path synthesis problem for four-bar linkages, Journal of Mechanical Design, Transactions of the ASME, 114(1) (1992) 153-159.

[19] S.K. Acharyya, M. Mandal, Performance of EAs for four-bar linkage synthesis, Mechanism and Machine Theory, 44(9) (2009) 1784-1794.

[20] J. Buśkiewicz, Reduced number of design parameters in optimum path synthesis with timing of four-bar linkage, Journal of Theoretical and Applied Mechanics (Poland), 56(1) (2018) 43-55.

[21] W.Y. Lin, A GA-DE hybrid evolutionary algorithm for path synthesis of four-bar linkage, Mechanism and Machine Theory, 45(8) (2010) 1096-1107.

[22] F.T. Sánchez Marín, A.P. González, Global optimization in path synthesis based on design space reduction, Mechanism and Machine Theory, 38(6) (2003) 579-594.

[23] S. Damangir, Optimum Synthesis of Mechanisms For Path Generation Using a New Curvature Based – Deflection Based Objective Function, (December) (2006) 672-676.

[24] D.H. Ham, W.C. Yoon, Genetic Algorithms in Mechanism Synthesis, Reliability Engineering & System Safety, 73 (2001).

[25] A.G. Erdman, Modern kinematics : developments in the last forty years, (1993) 604-604.

[26] S. Kota, S.J. Chiou, Use of orthogonal arrays in mechanism synthesis, Mechanism and Machine Theory, 28(6) (1993) 777-794.

[27] A. Smaili, N. Diab, A new approach to shape optimization for closed path synthesis of planar mechanisms, Journal of Mechanical Design, Transactions of the ASME, 129(9) (2007) 941-948.

[28] I. Ullah, S. Kota, Optimal synthesis of mechanisms for path generation using fourier descriptors and global search methods, Journal of Mechanical Design, Transactions of the ASME, 119(4) (1997) 504-510.

[29] G. Bovi, M. Rabuffetti, P. Mazzoleni, M. Ferrarin, A multiple-task gait analysis approach: Kinematic, kinetic and EMG reference data for healthy young and adult subjects, Gait and Posture, 33(1) (2011) 6-13.

[30] G. Abbasnejad, J. Yoon, H. Lee, Optimum kinematic design of a planar cable-driven parallel robot with wrench-closure gait trajectory, Mechanism and Machine Theory, 99 (2016) 1-18.

[31] K. Kora, J. Stinear, A. McDaid, Design, analysis, and

optimization of an acute stroke gait rehabilitation device, Journal of Medical Devices, Transactions of the ASME, 11(1) (2017) 014503-014503.

[32] Z. Ji, Y. Manna, Synthesis of a pattern generation mechanism for gait rehabilitation, Journal of Medical Devices, Transactions of the ASME, 2(3) (2008) 031004-031004.

HOW TO CITE THIS ARTICLE

A. Vali, M. R. Haghjoo, B. Beigzadeh, Synthesis of a Six-Link Mechanism for Generating the Ankle Motion Trajectory Using Shadow Robot Control Method, AUT J. Mech Eng., 6(2) (2022) 189-200.

DOI: 10.22060/ajme.2021.20455.6004